Letters

Dynamic AC Line Frequency Response Method for LUT-Based Variable On-Time Control in 360–800 Hz CRM Boost PFC Converter

Yu Wu, *Student Member, IEEE*, Xiaoyong Ren, *Member, IEEE*, Yuting Zhou, *Student Member, IEEE*, Qianhong Chen, *Member, IEEE*, and Zhiliang Zhang, *Senior Member, IEEE*

***Abstract*—To improve the input current total harmonic distortion (THD), the look-up table (LUT) method is used in the 360–800 Hz critical conduction mode (CRM) boost power factor correction (PFC) converter. When the ac line frequency changes drastically and suddenly, the zero-crossing detection method needs the half ac line period to follow the sudden frequency jump, causing a mismatching between the LUT and the ac line frequency. This mismatching in the time domain leads to a large current spike in the input current and even destruction in the PFC converter under some severe conditions. In this letter, a dynamic ac line frequency response method is proposed to eliminate this mismatching. The proposed method only needs to sample the input voltage, leading to a good performance in following the sudden frequency jump in a wide input voltage range. The effectiveness of the proposed method is verified with a 160 W GaN-based CRM boost PFC converter.**

***Index Terms*—Dynamic ac line frequency response, look-up table (LUT), variable on-time (VOT).**

I. Introduction

DUE to its simple control and low switching loss, the critical conduction mode (CRM) boost power factor correction (PFC) converter is widely used in low-to-mid power applications [1]–[5]. By realizing the valley switching (VS) and the zero-voltage switching (ZVS), the switching loss is minimized [6]–[8]. However, the VS and the ZVS lead to a negative inductor current, which causes the input current distortion near the zero-crossing input voltage [9]–[11].

To improve the input current total harmonic distortion, variable on-time (VOT) control methods are developed, which can be divided into two categories. One is the real-time calculation method [10], [11], and the other one is the look-up table (LUT) method [12]–[14]. The real-time calculation method can adaptively adjust the on-time with different input voltage and output load, but the accuracy is limited by the microprogrammed control unit (MCU) [10]. The LUT method can obtain the on-time by prestoring several LUTs, which means that the on-time can be calculated by a more accurate and complicated model [13], [14]. However, the LUT method is hard to realize the adaptability with different input voltage and output load. The situation becomes worse in the 360–800 Hz CRM boost PFC converter, which exists a wide ac line frequency working range.

The 360–800 Hz CRM boost PFC converter is used in the in-seat power supply, in which the output power changes from tens of to hundreds of watts [15]. According to the DO-160G, the 360–800 Hz CRM boost PFC converter is designated as category A(wide frequency, WF), which exists normal and abnormal frequency variations. The frequency variations can be up to 400 Hz/s due to the quick engine speed changes more particularly during engine runaway or failure mode scenarios.

In this letter, the impact of the sudden frequency jump on the LUT-based VOT control is analyzed. To minimize the current spike caused by the sudden frequency jump, a dynamic ac line frequency response method is proposed. By sampling the input voltage, the proposed method can follow the sudden frequency jump immediately in a wide input voltage range. A 160-W GaN-based CRM boost PFC converter is built to verify the effectiveness of the proposed method. The experimental results show that the proposed method can follow the sudden frequency jump fleetly, even under the worst situation that the ac line frequency jumps from 800 to 360 Hz.

II. Impact of the Sudden Frequency Jump

To discuss the impact of the sudden frequency jump, the implementation of the LUT-based VOT control is illustrated in this section first. Then, the mismatching between the ac line frequency f_l and the LUT, and its impact on the PFC converter are analyzed.

A. Implementation of the LUT-Based VOT Control

To illustrate the implementation of the LUT-based VOT control, Fig. 1 shows the system diagram. In which, v_{in} is the input voltage, L_b is the boost inductor, C_{in} and C_o are the input and output filter capacitor, respectively, Q_b is the power switch, D_b is the freewheeling diode, and R_o is the output resistor.

Manuscript received September 28, 2020; revised November 3, 2020; accepted November 18, 2020. Date of publication November 23, 2020; date of current version February 5, 2021. This work was supported in part by the Natural Science Foundation of China under Grants 51677086 and 51777093, and in part by the by Industrial Prospective and Key Core Technology Funding of Jiangsu Province under Grant BE2019113. *(Corresponding author: Xiaoyong Ren.)*

The authors are with the Aero-Power Sci-Tech Center, Department of Electrical Engineering, Nanjing University of Aeronautics and Astronautics, Nanjing 210016, China (e-mail: wuyu1995@nuaa.edu.cn; renxy@nuaa.edu.cn; zyt0624@nuaa.edu.cn; chenqh@nuaa.edu.cn; zlzhang@nuaa.edu.cn).

Color versions of one or more of the figures in this article are available at https://doi.org/10.1109/TPEL.2020.3039861.

Digital Object Identifier 10.1109/TPEL.2020.3039861

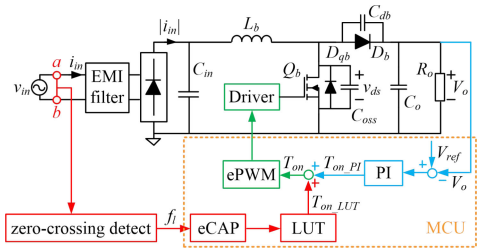

Fig. 1. System diagram of the LUT-based VOT control.

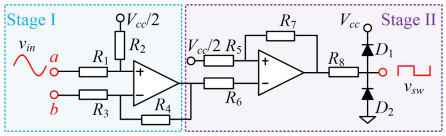

Fig. 2. ZCD circuit built by the operational amplifier.

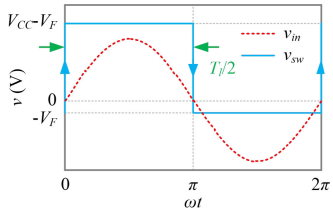

Fig. 3. Mapping relationship between the square-wave signal and $v_{\rm in}$.

As shown in Fig. 1, the whole system consists of four parts, the main circuit, the driver circuit, the zero-crossing detection (ZCD) circuit, and the MCU. The ZCD circuit obtains f_l and the zero-crossing point, which determines the choice of $T_{\rm on\_LUT}$. Due to the limitation of the storage space in MCU, the LUT is established under the light load condition. Then, to cover all the power range, a proportional-integral (PI) controller is added to keep the output voltage V_o equal to the reference voltage $V_{\rm ref}$. Thus, the ON-time $T_{\rm on}$ can be obtained by the sum of $T_{\rm on\_LUT}$ and $T_{\rm on\_PI}$ from the LUT and the PI controller.

Normally, the ZCD circuit is built by the operational amplifier as shown in Fig. 2, which consists of two stages. Stage I provides a noninverting attenuation with positive offset for $v_{\rm in}$, ensuring that $v_{\rm in}$ is in the input voltage range of the operational amplifier. Stage II is a hysteresis comparator, transferring the ac signal into the square-wave signal $v_{\rm sw}$ for the MCU.

By detecting the square-wave signal, the MCU can obtain f_l and the zero-crossing point. To illustrate the principle, Fig. 3 shows the mapping relationship between $v_{\rm sw}$ and $v_{\rm in}$, where V_F is the forward voltage of D_1 and D_2. By detecting the rising and falling edge of $v_{\rm sw}$, the zero-crossing point can be obtained. Moreover, f_l can be obtained by detecting the time interval between the rising and falling edge.

Since f_l changes from 360 to 800 Hz, the LUT-based VOT control should also adapt to different f_l conditions. Taking the LUT established by f_{l1}, LUT$_{fl1}$, as the reference value, $T_{\rm on\_LUT}$ required for f_{l2} can be expressed as follows:

$$T_{\rm on\_LUT} = {\rm LUT}_{fl1}\left({\rm INT}\left(\frac{mf_{l2}}{f_s}n\right)\right) \tag{1}$$

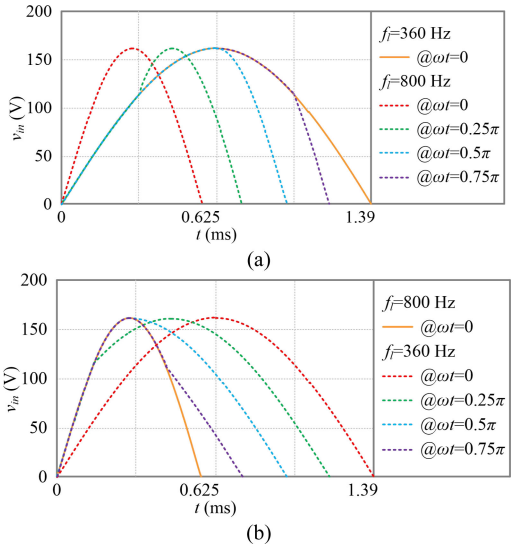

Fig. 4. Expected $v_{\rm in}$ at four typical points. (a) 360→800 Hz. (b) 800→360 Hz.

where INT(x) is the integer-valued function, f_s is the sampling frequency, m is the total number of the array element in LUT$_{f1l}$, and n is the trigger times of the sampling interrupt.

Normally, n is reset to be 1 once the zero-crossing point is detected by the MCU. Thus, both f_l and n determine $T_{\rm on\_LUT}$ as given in (1), realizing the LUT-based VOT control.

B. Impact of the Sudden Frequency Jump

As discussed earlier, $T_{\rm on\_LUT}$ is determined by the detected f_l, the detected zero-crossing point, and the prestored LUT. From Fig. 3, it can be noted that the detected f_l requires the half ac line period, $0.5T_l$, to follow the variation of the actual f_l, causing a mismatching between the LUT and f_l. The worst situation occurs when f_l jumps from 360 to 800 Hz, or, conversely, from 800 to 360 Hz.

Since f_l can change at any point during the half ac line period, four typical points are used to analyze the impact, including $\omega t = 0$, 0.25π, 0.5π, and 0.75π. The expected $v_{\rm in}$ at four typical points is shown in Fig. 4.

1) f_l Jumps From 360 to 800 Hz: As shown in Fig. 4(a), with the jump point increasing, the deviation between $v_{\rm in}$ with $f_l =$ 360 Hz and that with $f_l =$ 800 Hz decreases, which means that the impact caused by the sudden frequency jump is reduced. Using the calculation model in [14], Fig. 5(a) shows the distribution of the required and the given $T_{\rm on\_LUT}$ in the time domain. Then, the expected input current $i_{\rm in}$ can be illustrated in Fig. 5(b).

From Fig. 5(a), it can be noted that the sudden frequency jump causes a mismatching between the LUT and f_l, causing the nonsinusoidal $i_{\rm in}$ in Fig. 5(b).

When f_l jumps at $\omega t = 0$, there exists a crossover point between the given $T_{\rm on\_LUT}$ and the required one. Thus, before the crossover point, the given $T_{\rm on\_LUT}$ is larger than the required one, resulting in a current spike in $i_{\rm in}$. After the crossover point, the given $T_{\rm on\_LUT}$ is smaller than the required one, causing a zero-current platform in $i_{\rm in}$.

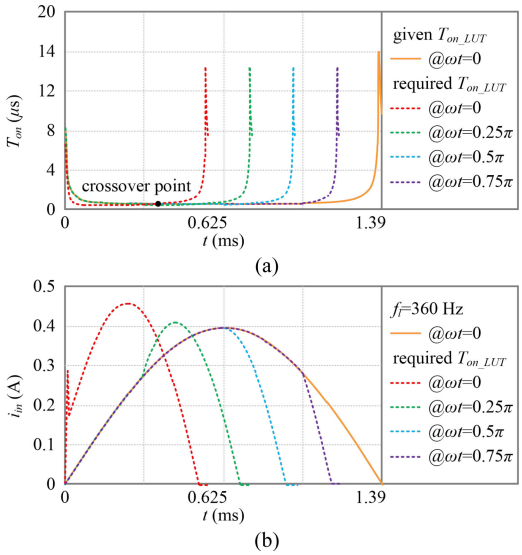

Fig. 5. Expected waveforms under the condition that f_l jumps from 360 to 800 Hz. (a) Distribution of $T_{\mathrm{on\_LUT}}$. (b) Expected i_{in}.

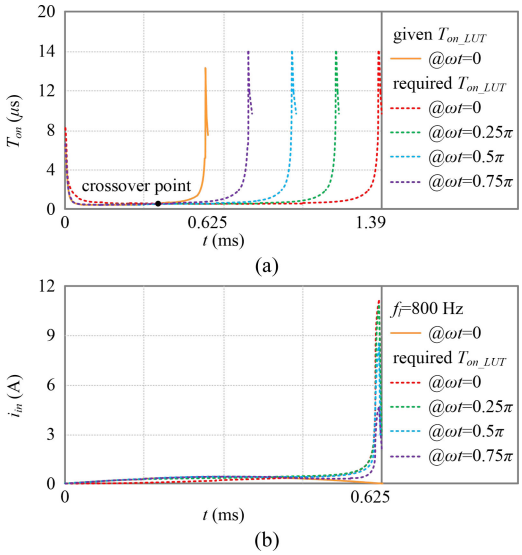

Fig. 6. Expected waveforms under the condition that f_l jumps from 800 to 360 Hz. (a) Distribution of $T_{\mathrm{on\_LUT}}$. (b) Expected i_{in}.

Different from the situation that $\omega t = 0$, the given $T_{\mathrm{on\_LUT}}$ of the other three situations is always no larger than the required one. Thus, there exists a zero current platform in i_{in}, while no current spike.

2) f_l Jumps From 800 to 360 Hz: Similar to the analysis mentioned above, Fig. 6(a) shows the distribution of the required and the given $T_{\mathrm{on\_LUT}}$ in the time domain. Then, the expected i_{in} can be illustrated in Fig. 6(b).

From Fig. 6(a), it can be noted that there exists a crossover point between the given $T_{\mathrm{on\_LUT}}$ and the required one. After the crossover point, the largest $T_{\mathrm{on\_LUT}}$ is given at a large v_{in}, causing a current spike, which is large enough to destroy the PFC converter. Thus, a method is required to minimize the current spike for practical application.

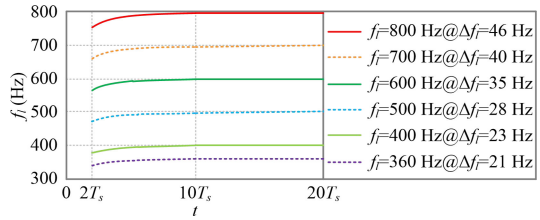

Fig. 7. Calculation results of f_l in ($2T_s$, $20T_s$).

III. Dynamic AC Line Frequency Response Method

To minimize the current spike caused by the mismatching when f_l changes drastically and suddenly, a method is required to follow the sudden frequency jump fleetly.

A. Dynamic AC Line Frequency Response Method

To simplify the analysis, define v_{in} as follows:

$$v_{\mathrm{in}}(t) = \sqrt{2} V_{\mathrm{in}} \sin(2\pi f_l t) \tag{2}$$

where V_{in} is the root mean square (rms) of v_{in}.

According to the equivalent infinitesimal, $\sin(2\pi f_l t)$ and $2\pi f_l t$ converge to zero at the same point $t = 0$, which means that

$$\lim_{t\to 0} \frac{\sin(2\pi f_l t)}{2\pi f_l t} = 1. \tag{3}$$

That is, near the zero-crossing point, v_{in} can be rewritten as (4). In which, v_{in} can be obtained by the sampling circuit, t can be obtained by the MCU, while V_{in} and f_l are unknown under the abnormal operating conditions. According to the DO-160G, V_{in} can change from 97 to 134 VAC, which makes it hard to calculate f_l by (4) directly

$$v_{\mathrm{in}}(t) = 2\sqrt{2}\pi V_{\mathrm{in}} f_l t. \tag{4}$$

To eliminate the impact of V_{in}, the derivative of v_{in} is analyzed in the discrete-time domain, which can be expressed as follows:

$$\begin{aligned} \frac{dv_{\mathrm{in}}(nT_s)}{dt} &= 2\sqrt{2}\pi V_{\mathrm{in}} f_l \cos(2\pi f_l n T_s) \\ &= \frac{v_{\mathrm{in}}((n+1)T_s) - v_{\mathrm{in}}((n-1)T_s)}{2T_s} \end{aligned} \tag{5}$$

where T_s is the sampling time and equal to $1/f_s$.

Substituting (4) into (5), f_l can be expressed as follows:

$$f_l = \frac{1}{2\pi n T_s} \arccos\left(\frac{t_0\left(v_{\mathrm{in}}((n+1)T_s) - v_{\mathrm{in}}((n-1)T_s)\right)}{2T_s v_{\mathrm{in}}(t_0)}\right) \tag{6}$$

where t_0 is a time near the zero-crossing point, which is chosen to be $2T_s$ in this letter.

Let f_s be 250 kHz, then T_s is 4 μs. Using (6), Fig. 7 shows the calculation results of f_l in ($2T_s$, $20T_s$). From the figure, it can be noted that relative error δf_l is smaller than 6% at $t = 2T_s$, and δf_l is smaller than 0.5% at $t = 10T_s$, implying the accuracy of the proposed dynamic ac line frequency response method.

B. Implementation of the Proposed Method

As analyzed earlier, the proposed dynamic ac line frequency response method can follow f_l fleetly near the zero-crossing point regardless of V_{in}. However, f_l can change at any point during the half ac line period, as discussed in Section II. Thus, the implementation of the proposed method needs to be improved

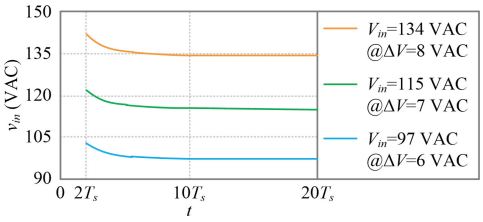

Fig. 8. Calculation results of $V_{\rm in}$ in ($2T_s$, $20T_s$).

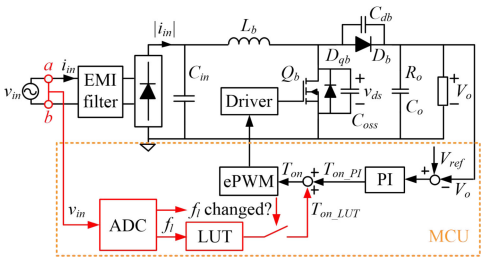

Fig. 9. System diagram of the proposed method.

to avoid the destruction of the PFC converter caused by the sudden frequency jump in ($20T_s$, $0.5T_l$).

Near the zero-crossing point, substituting (6) into (4), $V_{\rm in}$ can be expressed as follows:

$$V_{\rm in} = \frac{n v_{\rm in}(2T_s)}{2\sqrt{2}\arccos\left(\frac{v_{\rm in}((n+1)T_s)-v_{\rm in}((n-1)T_s)}{v_{\rm in}(2T_s)}\right)}. \quad (7)$$

Using (7), Fig. 8 shows the calculation results of $V_{\rm in}$ in ($2T_s$, $20T_s$). From the figure, it can be noted that $\delta V_{\rm in}$ is smaller than 7% at $t = 2T_s$, and $\delta V_{\rm in}$ is smaller than 0.5% at $t = 10T_s$. Thus, the proposed method can also obtain $V_{\rm in}$ fleetly near the zero-crossing point.

That is, near the zero-crossing point, the initial f_l and $V_{\rm in}$ can be obtained immediately, making it easy to predict the value of $v_{\rm in}$ at any point during the half ac line period. Once f_l changes, the sampled $v_{\rm in}$ will deviate from the predicted one as shown in Fig. 4. After detecting the variation of f_l, $T_{\rm on\_LUT}$ is gradually reduced to zero by the MCU, changing the control mode from the VOT mode into the COT mode. Thus, the current spike in Figs. 5(b) and 6(b) can be avoided.

Based on the proposed method, Fig. 9 shows the system diagram for the MCU implementation. The ADC module samples $v_{\rm in}$ in real-time. Near the zero-crossing point, the initial f_l and $V_{\rm in}$ of the current period are obtained to check the variation of f_l. If f_l is unchanged during ($20T_s$, $0.5T_l$), the control mode keeps the VOT mode. Then, $T_{\rm on\_LUT}$ is obtained by (1) and $T_{\rm on\_PI}$ is obtained by the PI controller. The required $T_{\rm on}$ can be calculated by the sum of $T_{\rm on\_LUT}$ and $T_{\rm on\_PI}$. If f_l is changed during ($20T_s$, $0.5T_l$), the control mode is changed into the COT mode, avoiding the current spike. Then, the required $T_{\rm on}$ can be calculated by $T_{\rm on\_PI}$. In the next half ac line period, repeat the abovementioned operation.

IV. Experimental Results

The experimental work is conducted with a 160-W CRM boost PFC converter. The circuit parameters are given in Table I.

TABLE I
Circuit Parameters of the Experimental Prototype

Input voltage	115 VAC	C_r	56 pF
Output voltage	270 VDC	L_b	101 μH
Max output power	160 W	C_{in}	100 nF
Power switch Q_b	TPH3206PS	C_{out}	180 μF/ 450 VDC
Boost diode D_b	C3D02060A	MCU	TMS320F28335

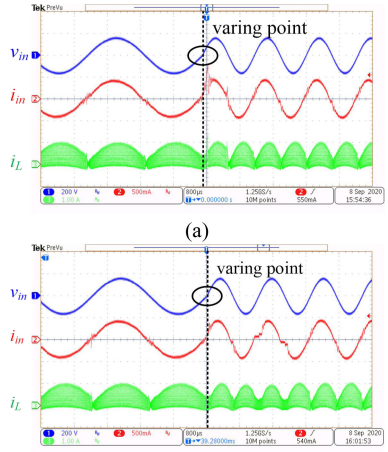

Fig. 10. Dynamic response with 20% load (360→800 Hz) near the zero-crossing point: (a) without the proposed method; (b) with the proposed method.

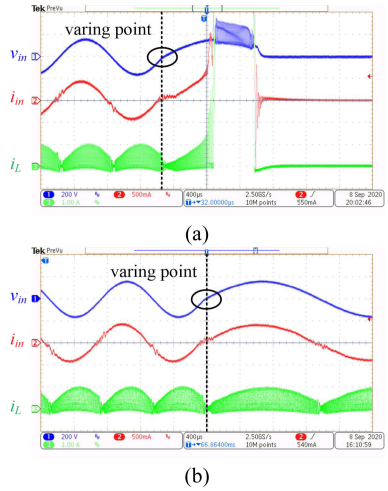

Fig. 11. Dynamic response with 20% load (800→360 Hz) near the zero-crossing point: (a) without the proposed method; (b) with the proposed method.

Under the condition that f_l jumps from 360 to 800 Hz near the zero-crossing point, Fig. 10 shows the dynamic response without and with the proposed dynamic ac line frequency response method. From Fig. 10(a), it can be noted that there exists a current spike in $i_{\rm in}$, which is in coincidence with the expected waveforms in Fig. 5(b). By using the proposed method, Fig. 10(b) shows that the MCU can follow the sudden frequency jump fleetly, eliminating the current spike.

Similarly, the dynamic experiments are conducted under the condition that f_l jumps from 800 to 360 Hz near the zero- crossing point, which is shown in Fig. 11. Same as the analysis in

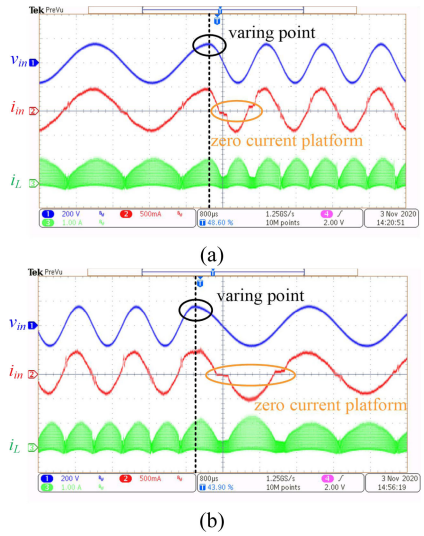

Fig. 12. Dynamic response under the frequency variation with 20% load near the peak voltage point: (a) 360→800 Hz; (b) 800→360 Hz.

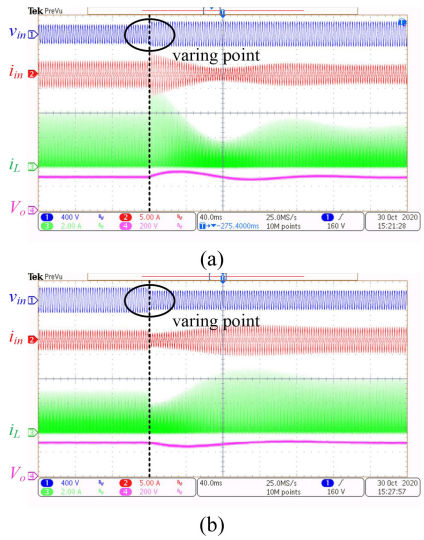

Fig. 13. Dynamic response under the voltage variation with full load. (a) 97→134 Vac. (b) 134→97 Vac.

Section II, the mismatching between the LUT and f_l makes the largest $T_{\text{on\_LUT}}$ appear at a large v_{in}, causing a current spike, which is large enough to destroy the PFC converter. By using the proposed method, Fig. 11(b) shows that the MCU can follow the sudden frequency jump fleetly, avoiding the destruction of the PFC converter.

Since f_l can change at any point during the ac line period, the dynamic experiments are also conducted near the peak voltage point, which is shown in Fig. 12. As shown in the figure, once the variation of f_l is detected, the control mode is changed into the COT mode, leading to a zero current platform near the zero-crossing point. In the next half ac line period, the control mode recovers to the VOT mode, eliminating the zero current platform, which is in coincidence with the implementation in Section III.

To verify the effectiveness of the proposed method with different V_{in}, the dynamic experiments are also conducted under the condition that V_{in} jumps between 97 and 134 Vac. As shown in Fig. 13, there exists no current spike in i_{in}, which means that the variation of V_{in} has no impact on the detection of f_l. That is, the proposed method can handle the situation with different V_{in}.

V. Conclusion

This letter presents a dynamic ac line frequency response method for 360–800 Hz CRM boost PFC converters. The impact of the sudden ac line frequency jump on the LUT-based VOT control is analyzed. To minimize the current spike caused by the mismatching when f_l changes drastically and suddenly, a dynamic ac line frequency response method is proposed. By sampling the input voltage, the proposed method can follow the sudden frequency jump immediately in a wide input voltage range. The experimental results show that the proposed method can follow the sudden frequency jump fleetly, even under the worst situation that the ac line frequency jumps from 800 to 360 Hz.

References

[1] K. Yao *et al.*, "Optimal switching frequency variation range control for CRM boost PFC converter," *IEEE Trans. Ind. Electron.*, vol. 68, no. 2, pp. 1197–1209, Feb. 2021.

[2] Y. Chen and Y. Chen, "Line current distortion compensation for DCM/CRM boost PFC converters," *IEEE Trans. Power Electron.*, vol. 31, no. 3, pp. 2026–2038, Mar. 2016.

[3] K. Yao, Z. Zhang, J. Yang, J. Liu, J. Li, and F. Shao, "Quasi-fixed switching frequency control of CRM boost PFC converter based on variable inductor in wide input voltage range," *IEEE Trans. Power Electron.*, vol. 36, no. 2, pp. 1814–1827, Feb. 2021.

[4] Q. Ji, X. Ruan, and Z. Ye, "The worst conducted EMI spectrum of critical conduction mode boost PFC converter," *IEEE Trans. Power Electron.*, vol. 30, no. 3, pp. 1230–1241, Mar. 2015.

[5] Y. S. Roh, Y. J. Moon, J. Park, and C. Yoo, "A two-phase interleaved power factor correction boost converter with a variation-tolerant phase shifting technique," *IEEE Trans. Power Electron.*, vol. 29, no. 2, pp. 1032–1040, Feb. 2014.

[6] K. De Gusseme, W. R. Ryckaert, D. M. Van de Sype, J. A. Ghijselen, J. A. Melkebeek, and L. Vandevelde, "A boost PFC converter with programmable Har monic resistance," *IEEE Trans. Ind. Appl.*, vol. 43, no. 3, pp. 742–750, May/Jun. 2007.

[7] X. Ren, Y. Zhou, Z. Guo, Y. Wu, Z. Zhang, and Q. Chen, "Simple analog-based accurate variable on-time control for critical conduction mode boost power factor correction converters," *IEEE J. Emerg. Sel. Top. Power Electron.*, vol. 8, no. 4, pp. 4025–4036, Dec. 2020.

[8] W. Cheng, J. Song, H. Li, and Y. Guo, "Time-varying compensation for peak current-controlled PFC boost converter," *IEEE Trans. Power Electron.*, vol. 30, no. 6, pp. 3431–3437, Jun. 2015.

[9] L. Huber, B. T. Irving, and M. M. Jovanovic, "Effect of valley switching and switching-frequency limitation on line-current distortions of DCM/CCM boundary boost PFC converters," *IEEE Trans. Power Electron.*, vol. 24, no. 2, pp. 339–347, Feb. 2009.

[10] X. Ren, Y. Wu, Z. Guo, Z. Zhang, and Q. Chen, "An online monitoring method of circuit parameters for variable on-time control in CRM boost PFC converters," *IEEE Trans. Power Electron.*, vol. 34, no. 2, pp. 1786–1797, Feb. 2019.

[11] J. W. Kim, H. S. Youn, and G. W. Moon, "A digitally controlled critical mode boost power factor corrector with optimized additional on time and reduced circulating losses," *IEEE Trans. Power Electron.*, vol. 30, no. 6, pp. 3447–3456, Jun. 2015.

[12] X. Ren, Z. Guo, Y. Wu, Z. Zhang, and Q. Chen, "Adaptive LUT-based variable on-time control for CRM boost PFC converters," *IEEE Trans. Power Electron.*, vol. 33, no. 9, pp. 8123–8136, Sep. 2018.

[13] X. Ren, Y. Zhou, Z. Guo, Y. Wu, Z. Zhang, and Q. Chen, "Analysis and improvement of capacitance effects in 360–800 Hz variable on-time controlled CRM boost PFC converters," *IEEE Trans. Power Electron.*, vol. 35, no. 7, pp. 7480–7491, Jul. 2020.

[14] X. Ren, Y. Wu, Z. Zhang, and Q. Chen, "Accurate operation analysis based variable on-time control for 360–800 Hz CRM boost PFC converters," *IEEE Trans. Ind. Electron.*, vol. 67, no. 8, pp. 6845–6853, Aug. 2020.

[15] *1191-41, -46 (3 Output) 110 VAC and High Power USB In-Seat Power Supply*, Astronics corporation, East Aurora, NY, USA, Datasheet, 2018.